Myosin Heavy Chain 10 (MYH10) Gene Silencing Reduces Cell Migration and Invasion in the Glioma Cell Lines U251, T98G, and SHG44 by Inhibiting the Wnt/β-Catenin Pathway

Authors' Contribution:
Study Design A
Data Collection B
Statistical Analysis C
Data Interpretation D
Manuscript Preparation E
Literature Search F
Funds Collection G

AB 1 Yang Wang*
AB 2 Qi Yang*
CD 3 Yanli Cheng
DE 4 Meng Gao
CE 5 Lei Kuang
EF 6 Chun Wang

1 Department of Neurosurgery, 2nd Ward, Taihe Hospital, Shiyan, Hubei, P.R. China
2 Department of Orthopedic Surgery, 3rd Ward, Taihe Hospital, Shiyan, Hubei, P.R. China
3 Skin Department, Taihe Hospital, Shiyan, Hubei, P.R. China
4 Department of Ophthalmology and Otolaryngology, Weifang Maternal and Child Health Care Hospital, Weifang, Shandong, P.R. China
5 Department of Neurosurgery, 3rd Ward, Taihe Hospital, Shiyan, Hubei, P.R. China
6 Department of Neurosurgery, Suizhou Central Hospital, Suizhou, Hubei, P.R. China

* These authors contributed equally to this work

Corresponding Author: Chun Wang, e-mail: chunw_wangc@163.com
Source of support: Departmental sources

Background: The myosin heavy chain 10 or MYH10 gene encodes non-muscle myosin II B (NM IIB), and is involved in tumor cell migration, invasion, extracellular matrix (ECM) production, and epithelial-mesenchymal transition (EMT). This study aimed to investigate the effects of the MYH10 gene on normal human glial cells and glioma cell lines in vitro, by gene silencing, and to determine the signaling pathways involved.

Material/Methods: The normal human glial cell line HEB, and the glioma cell lines, U251, T98G, and SHG44 were studied. Plasmid transfection silenced the MYH10 gene. The cell counting kit-8 (CCK-8) assay evaluated cell viability. Cell migration and invasion were evaluated using scratch and transwell assays. Western blot measured the protein expression levels, and quantitative real-time polymerase chain reaction (qRT-PCR) was used to detect the mRNA expression levels, for MYH10, metastasis-associated protein 1 (MTA-1), matrix metalloproteinase (MMP)-1, MMP-9, tissue inhibitor of metalloproteinases 2 (TIMP2), collagen 1, E-cadherin, vimentin, Wnt3a, β-catenin, and cyclin D1.

Results: The MYH10 gene was overexpressed in U251, T98G, and SHG44 cells. MYH10 expression was down-regulated following siMYH10 plasmid interference, which also inhibited glioma cell migration and invasion. MYH10 gene silencing resulted in reduced expression of MTA-1, MPP-2, MMP-9 and vimentin, and increased expression of TIMP-2, E-cadherin and collagen 1 at the protein and mRNA level, and inhibited the Wnt/β-catenin pathway.

Conclusions: In human glioma cell lines, silencing the MYH10 gene reduced cell migration and invasion, by inhibiting the Wnt/β-catenin pathway, which may regulate the ECM and inhibit EMT in human glioma.

MeSH Keywords: Cell Migration Inhibition • Epithelial-Mesenchymal Transition • Glioma • Myosin Heavy Chains • Neoplasm Invasiveness

Full-text PDF: https://www.medscimonit.com/abstract/index/idArt/911523

📄 3345   ⊞ 1   📊 4   📚 47

Background

The malignant form of glioma, glioblastoma, is the most common primary malignant tumor of the brain, comprising 16% of all primary tumors of the brain and central nervous system (CNS) [1]. It is challenging to treat malignant gliomas, due to their high recurrence rate and low survival rate [2]. Currently, the main methods of treatment include radiotherapy, chemotherapy or surgery [1,3]. However, due to the special location of these tumors, there are limitations in the use of radiotherapy and chemotherapy, which may be associated with side effects that limit the patient's tolerance to these treatments [4]. Because malignant gliomas are highly invasive and the tumor borders may not be clear, surgical resection is also difficult [5]. Therefore, there are several ongoing studies to study the pathogenesis of malignant glioma, including the mechanisms involved in tumor invasion, and to identify new therapeutic targets.

The myosin heavy chain 10 or MYH10 gene encodes non-muscle myosin II B (NM IIB) and is involved in tumor cell migration, invasion, extracellular matrix (ECM) production, and epithelial-mesenchymal transition (EMT). The MYH10 gene is located on human chromosome 17, and the encoded protein, NM IIB, is mainly present in nerve cells, megakaryocytes, and other non-muscle cells [6,7]. NM IIB has a role in cell adhesion and migration [8]. A previously published study showed that the MYH10 gene was overexpressed in breast cancer and that increased expression of MYH10 was associated with tumor cell invasion in breast cancer [9]. A previously published study also showed that mutations in the MYH10 gene promoted cell migration and were associated with metastasis of malignant tumors [10]. However, there have been no previously published studies on the effect of MYH10 gene expression on the invasive properties of human glioma cells.

Cell migration and invasion are characteristics of tumor cells *in vitro* [11]. The invasion and migration of tumor cells *in vivo* is associated with the components of the extracellular matrix (ECM) and the effects of epithelial-mesenchymal transition (EMT) [11]. ECM and EMT are regulated by several signaling pathways [12,13]. Importantly, overexpression of the Wnt/β-catenin pathway has been shown to be associated with metastasis of several types of malignancy [14–16]. RNA interference technology is an effective method to study the function of genes and has demonstrated benefits in the rapid discovery of effective targets of drug action, confirmed by *in vitro* cell culture and other pre-clinical experimental techniques [17].

Therefore, the aim of this study was to investigate the effects of the MYH10 gene on normal human glial cells and glioma cell lines *in vitro*, by gene silencing, and to determine the effects on the expression of ECM and EMT-associated proteins and the Wnt/β-catenin pathway related proteins.

Material and Methods

Cells culture

The normal glial cell line, HEB, and the human glioma cell lines, U251, T98G, and SHG44, were purchased from Shanghai Beinuo Biotech Co., Ltd. Cells were cultured in Dulbecco's modified Eagle's medium (DMEM) including 10% fetal calf serum, penicillin and streptomycin 100 U/mL (HyClone Laboratories Inc., South Logan, UT, USA) in an incubator at 37°C in 5% CO_2.

MYH10 gene interference plasmid construction and transfection

The MYH10-small interfering RNA (siRNA) plasmid (Thermo Fisher Scientific, Waltham, MA, USA) was mixed with Lipofectin 2000, and OPTI-MEM™ reduced serum medium (Thermo Fisher Scientific, Waltham, MA, USA) at a ratio of 1: 2.5: 250 and allowed to stand for 20 min at room temperature to obtain a liposome mixture. MYH10-negative-siRNA (without the siRNA plasmid) (Thermo Fisher Scientific, Waltham, MA, USA) was used as the normal control (NC) group.

The T98G human glioma cell line was placed in a DMEM medium, cultured at 37°C in 5% CO_2, and seeded into a cell culture plate overnight. The inoculation density was 1×10^5 cells/mL. After removing of the cell culture medium, cells were added with 100 µL of the MYH10-siRNA-liposome mixture and the MYH10 without the siRNA plasmid liposome mixture respectively, and then cultured for 6 h. DMEM culture medium was added, and further culture was performed for 24 h. The cells were passaged at a ratio of 1: 10, cultured in 1 µg/mL puromycin media (Becton Dickinson, Franklin Lakes, NJ, USA) until a confluent clonal cell population was grown, at which time, cells were selected and seeded in 96-well cell culture plates. When the cells reached 70% confluence, they were transferred to culture flasks. Finally, three experimental groups of cells were obtained for further study: the MYH10-siRNA interference group (the siMYH10 group), the negative-siRNA interference group, without the siRNA plasmid (the NC group), and untransfected group (the NC or control group). The transfection efficiencies were detected using quantitative real-time polymerase chain reaction (RT-qPCR) and Western blot, respectively.

Cell viability using the cell counting kit-8 (CCK-8) assay

The cell counting kit-8 (CCK-8) assay (Tong Ren Tang Technologies Co Ltd, Beijing, China) was used to detect cell viability at 12 h, 24 h, and 48 h after plasmid transfection of the T98G cells. The cells were inoculated onto 96-well plates and pre-incubated at 37°C in 5% CO_2, and then 10 mL of CCK-8 reagent was added, and culture was continued at 37°C in 5% CO_2 for 4 h. The absorbance of each well at 450 nm

was measured by using an ELX 800 microplate reader (BioTek, Winooski, VT, USA), and cell viability was calculated according to the standard curve.

Scratch assay

A black marker pen was used to draw a horizontal line across each well of the 6-well plate. Each horizontal line had a fixed interval of 0.5 cm. Then, $5×10^5$ of viable cells were added to each well and incubated overnight at 37°C in 5% CO_2. The fusion rate achieved was 100%. After using the tip of the pipette perpendicular to the black line behind the plate to scratch the culture, the cells were gently washed with PBS buffer and incubated for 24 h in serum-free medium (Thermo Fisher Scientific, Waltham, MA, USA). After taking pictures, ImageJ software was used to process the images and calculate the cell mobility.

Transwell analysis

Transwell chamber and related reagents were purchased from Corning (New York, NY, USA). The cells were digested with trypsin for 5 min, and 500 mL of the cell culture was added in the lower chamber, and $5 × 10^4$ cells were added and cultured for 4 h. The cells from the upper chamber were added to the lower chamber. Finally, a cell suspension containing $5×10^4$ cells was added into the upper chamber vertically, dropwise, followed by culture for 6–8 h at 37°C and 5% CO_2. After staining with Giemsa (Shanghai Gefan Biotechnology Co., Ltd., China), five high-power fields were randomly selected using light microscopy to quantify the rate of cell invasion.

Quantitative real-time polymerase chain reaction (qRT-PCR) analysis

The cells were titrated and lysed using TRIzol (Takara, Minato-ku, Tokyo, Japan) at 0°C for 5 minutes. The RNAs were extracted using carbon tetrachloride (CCl_3) and dissolved in diethyl pyrocarbonate (DEPC) water (Sigma. RNA concentration was measured using a NanoDrop One Microvolume UV-Vis spectrophotometer (Thermo Fisher Scientific, Waltham, MA, USA), and electrophoresis detected no degradation in a 2% agarose gel. Reverse transcription assays were performed on RNA samples using a reverse transcription kit (Takara, Minato-ku, Tokyo, Japan) to synthesize cDNA. Reverse transcription reaction conditions were 37°C for 15 min and reverse transcriptase inactivation conditions were 85°C for 15 s.

RT-qPCR experiments were performed using the SYBR Prellix Ex Taq™ Real-Time PCR Kit (Takara, Minato-ku, Tokyo, Japan). PCR was performed by activating the DNA polymerase at 95°C for 5 min, followed by 40 cycles of a two-step PCR (95°C for 10 sec and 60°C for 30 sec) and a final extension at 75°C for 10 min and held at 4°C. DNase and RNase-free water were used

Table 1. The sequences of primers used in quantitative the real-time polymerase chain reaction (qRT-PCR).

Primer name	Sequence (5'-3')	Product size (bp)
MYH10-Forward	CGACGCGTGCCAACGCATC	371
MYH10-Reverse	GACACAGTTGATCTTTCAGGAAGG	
MTA-1-Forward	AGCTACGAGCAGCACAACGGGGT	298
MTA-1-Reverse	CACGCTTGGTTTCCCGAGGAT	
MMP-2-Forward	CAGCCCTGCAAGTTTCCATT	210
MMP-2-Reverse	GTTGCCCAGGAAAGTGAAGG	
MMP-9-Forward	GAGACTCTACACCCAGGACG	238
MMP-9-Reverse	GAAAGTGAAGGGGAAGACGC	
TIMP-1-Forward	AGACCACCTTATACCAGCGT	217
TIMP-1-Reverse	GCCACAAAACTGCAGGTAGT	
E-cadherin-Forward	TCCCATCAGCTGCCCAGAAA	321
E-cadherin-Reverse	ATTGTCCTTGTGTCCTCAGT	
Collagen I-Forward	CTTTGTACAACAGCACCCGC	247
Collagen I-Reverse	GTCAAAAGACAGCCACTCAGG	
Vimentin-Forward	CAGCCATGACCACCAGG	1401
Vimentin-Reverse	AAGGTCAAGACGTGCCAG	
Wnt3a-Forward	CAAGTCGGGTTCTTCTCTGGT	308
Wnt3a-Reverse	GTGATGCAAATAGGCAGCCG	
β-catenin-Forward	GGGTCCTCTGTGAACTTGCT	316
β-catenin-Reverse	AATCTTGTGGCTTGTCCTCA	
Cyclin D1-Forward	CTGGCCATGAACTACCTGGA	483
Cyclin D1-Reverse	GTCACACTTGATCACTCTGG-3	
GAPDH-Forward	CCATCTTCCAGGAGCGAGAT	222
GAPDH-Reverse	TGCTGATGATCTTGAGGCTG	

MYH10 – myosin heavy chain 10; MMP – matrix metalloproteinase; MTA-1 – metastasis-associated protein 1; TIMP – tissue inhibitor of metalloproteinases.

as the templates of negative control experiences. All primers were obtained from Genewiz (Suzhou, Jiangsu, China), and are listed in Table 1. GAPDH was used as an internal control. The formula $2^{-\Delta\Delta CT}$ was used to analyze the gene expression, as previously reported [18].

Western blot

Cells were lysed with liquid nitrogen and blocked with RIPA buffer (AbMole Bioscience, Houston, TX, USA), followed by 1% cleavage in phenylmethylsulfonyl fluoride (PMSF) and phosphatase inhibitors (AbMole Bioscience, Houston, TX, USA) and lysis for 30 min at 4°C. The supernatant was collected by centrifugation at 12,000 rpm for 4 minutes at 4°C. A standard curve was drawn using the bicinchoninic acid (BCA) method to determine the protein concentration. The kits were purchased from Kaiji Biotechnology Development Co., Ltd. (Nanjing, China). A 10% sodium dodecyl sulfate-polyacrylamide gel electrophoresis (SDS-PAGE) gel was prepared and the electrophoresis conditions were 80 V for 30 minutes. After completion of electrophoresis, the polyvinylidene difluoride (PVDF) membrane (Bio-Rad, Hercules, CA, USA) was transferred using a Trans-Blot Transfer Slot (Bio-Rad, Hercules, CA, USA) and the membrane was transferred at 350 mV at 0°C for about 100 minutes. The membrane was removed and labeled.

The following primary antibodies were obtained from Abcam (Cambridge, MA, USA): anti-MYH10 (Abcam, ab6759) (1: 1000); anti-MTA-1 (Abcam, ab226960) (1: 1000); anti-MMP-2 (Abcam, ab168864) (1: 1000); anti-MMP-9 (Abcam, ab38898) (1: 1000); anti-E-cadherin (Abcam, ab6528) (1: 800); anti-vimentin (Abcam, ab92547) (1: 800); anti-collagen I (Abcam, ab34710) (1: 800); anti-Wnt3a (Abcam, ab28472) (1: 700); anti-β-catenin, (Abcam, ab32572) (1: 800); anti-cyclin D1 (Abcam, ab134175) (1: 800). The following primary antibodies were obtained from R&D Systems (Minneapolis, MN, USA): anti-TIMP-2 (MAB971) (1: 500); anti-GAPDH (MAB5718 (1: 800). The primary antibodies were added to the membranes according to the kit instructions, shaking at room temperature for 2 h, then incubated at 4°C for 12 h.

The secondary antibodies were added and incubated at room temperature for 1.5 h: rabbit anti-mouse IgG (Abcam, ab99697) (1: 10000); goat anti-mouse IgG (Abcam, ab6785) (1: 8000); mouse anti-rabbit IgG (BA1034) (1: 7000) (Invitrogen, Carlsbad, CA, USA); donkey anti-rabbit IgG (NL004) (1: 5000) (R&D Systems, Minneapolis, MN, USA); mouse anti-rabbit IgG (BA1034) (1: 7000) (Invitrogen, Carlsbad, CA, USA). Chemiluminescence detection was carried out using the enhanced chemiluminescence (ECL) reagent (Huiying, Shanghai, China).

Statistical analysis

All the experimental data were presented as the mean ± standard deviation (SD). Statistical analysis was performed using SPSS version 20 (SPSS, Inc., Chicago, IL, USA). One-way analysis of variance (ANOVA) following Tukey's test was carried out to evaluate the differences between the experimental groups. Statistical significance was assumed to be a P-value <0.05.

Results

The expression level of the MYH10 gene in normal human glial cells and glioma cell lines

To compare the difference in MYH10 gene expression between the HEB normal human glial cells and human glioma cells, U251, T98G, and SHG44, real-time polymerase chain reaction (qRT-PCR) and Western blot were used to detect the expression level of MYH10 gene and protein. The MYH10 gene was expressed in both HEB and glioma cells, but the relative expression level of the MYH10 gene in U251, T98G, and SHG44 glioma cell lines were significantly greater when compared with the HEB cell line (P<0.05). The relative expression level of the MYH10 gene in T98G glioma cells was significantly increased when compared with the U251 and SHG44 glioma cell lines (P<0.05) (Figure 1A, 1B).

Effect of transfection with the short interfering (si)MYH10 plasmid on MYH10 gene expression in T98G human glioma cells

To study the transfection efficiency of MYH10 plasmids, quantitative real-time polymerase chain reaction (qRT-PCR) and Western blot were used. The results showed that MYH10 mRNA and protein expression levels decreased significantly after transfection (P<0.01) (Figure 2A, 2B). These findings confirmed that plasmid construction and transfection were successful.

Effect of transfection of siMYH10 plasmid on the viability of T98G human glioma cells

To investigate the effect of the siMYH10 plasmid transfection on cell viability of the T98G cell lines, the cell counting kit-8 (CCK-8) assay was used to examine the cell viability after transfection. Transfection experiments had no significant effect on cell viability within 48h (P>0.05) (Figure 2C). This finding indicated that plasmid transfection had no significant effect on the viability of T98G cells, indicating that plasmid transfection can study relevant cellular capabilities after MYH10 gene silencing.

Effects of siMYH10 on the migration and invasion ability of T98G human glioma cells

Scratch and transwell assays were used to detect the migration and invasion of T98G cells after MYH10 gene silencing. The results of this experiment showed that the migration and invasion of T98G cells in the siMYH10 group were significantly reduced compared with the NC group and the control group (P<0.05) (Figure 2D).
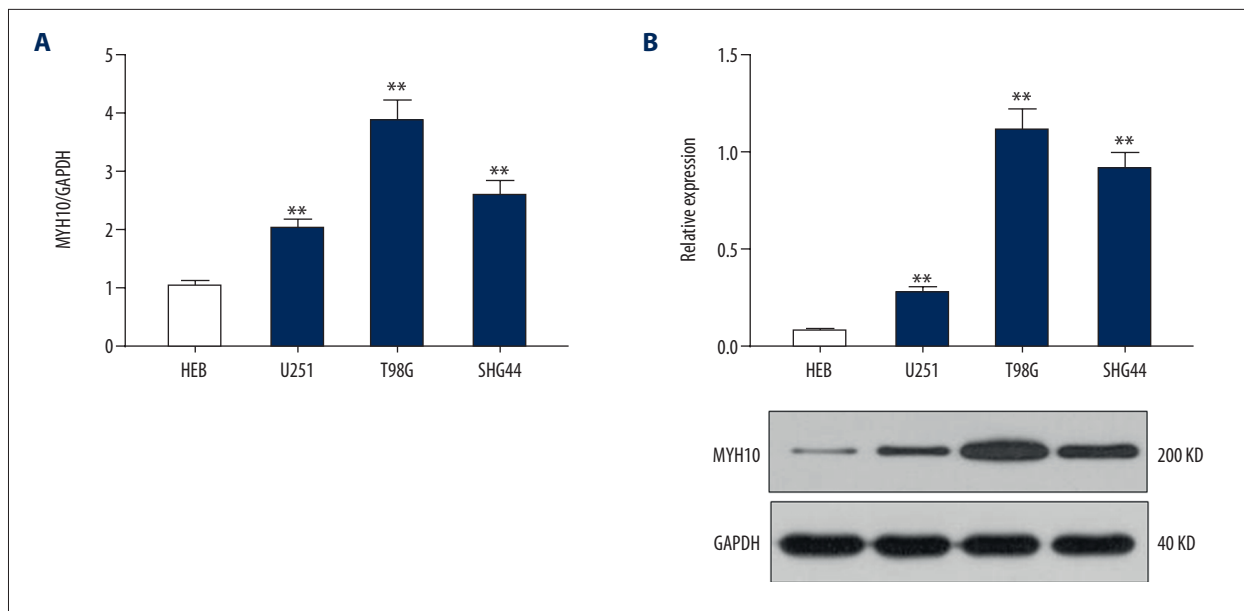
Figure 1. Expression of the MYH10 mRNA and protein in U251, T98G, and SHG44 glioma cell lines. (**A**) The mRNA level of MYH10 in the human brain glial cell line (HEB cells) and glioma cell lines (U251, T98G, and SHG44 cells) were detected by quantitative real-time polymerase chain reaction (qRT-PCR). (**B**) The proteins levels of MYH10 were measured by Western blot in the different cell lines. * $P<0.05$, ** $P<0.01$, compared with HEB cells. Data are shown as the mean ±SD (n=4).

Effects of siMYH10 on epithelial-mesenchymal transition (EMT) and extracellular matrix (ECM)-related gene expression in T98G human glioma cells

To investigate the basis for the cell invasion and migration, quantitative real-time polymerase chain reaction (qRT-PCR) and Westen blot were used to detect the expression of extra-cellular matrix (ECM) and epithelial-mesenchymal transition (EMT)-related mRNA and proteins. There was no significant difference between the NC group and the control group. For the four EMT-related genes, the expression levels of metas-tasis-associated protein 1 (MTA-1), matrix metalloproteinase (MMP)2, and MMP9 genes and proteins were significantly re-duced, while the expression of tissue inhibitor of metallopro-teinases 2 (TIMP2) genes and proteins was increased ($P<0.05$). For the three ECM-related genes, the expression levels of E-cadherin and collagen I mRNAs and proteins were upregu-lated, while the expression level of vimentin was down-regu-lated ($P<0.01$) (Figure 3A–3C).

Effects of siMYH10 on the expression of Wnt/β-catenin pathway genes in T98G human glioma cells

To investigate the mechanism of regulation of ECM and EMT after MYH10 silencing, the expression level of Wnt/β-catenin pathway related genes were studied. The results showed that the expression levels of Wnt3a, β-catenin, and cyclin D1 in the siMYH10 group were significantly lower compared with those of the NC group and the control group ($P<0.01$) (Figure 4A, 4B).

Discussion

The myosin heavy chain 10 or MYH10 gene encodes non-mus-cle myosin IIB (NM IIB) and is involved in tumor cell migration, invasion, the production of extracellular matrix (ECM) and in epithelial-mesenchymal transition (EMT). This study aimed to investigate the effects of the MYH10 gene on normal human glial cells and glioma cell lines *in vitro*, by gene silencing, and to determine the signaling pathways involved. Previous studies have shown that NM IIA and NM IIB can regulate cell move-ment by controlling cell polarization [19]. The findings of this study showed that the MYH10 gene was overexpressed in three glioma cell lines, U251, T98G, and SHG44, but that the expres-sion level of MYH10 in the T98G cell line was the highest, which is why this cell line was identified for further study.

Previously published studies have shown that the overexpres-sion of NM IIA protein was normal in many tumors [9,20]. NM IIA and NM IIB have a high degree of similarity, and studies have shown NM IIB is associated with malignant tumors [21], and that NM IIB is overexpressed in tumor cells [6]. By constructing an MYH10 interference plasmid and conducting transfection experiments, the expression level of the MYH10 gene was sig-nificantly reduced at 24 hours after transfection, but there was no significant effect on cell viability. This finding supported the success of the plasmid construction and transfection experi-ments and may provide a protocol for future studies.
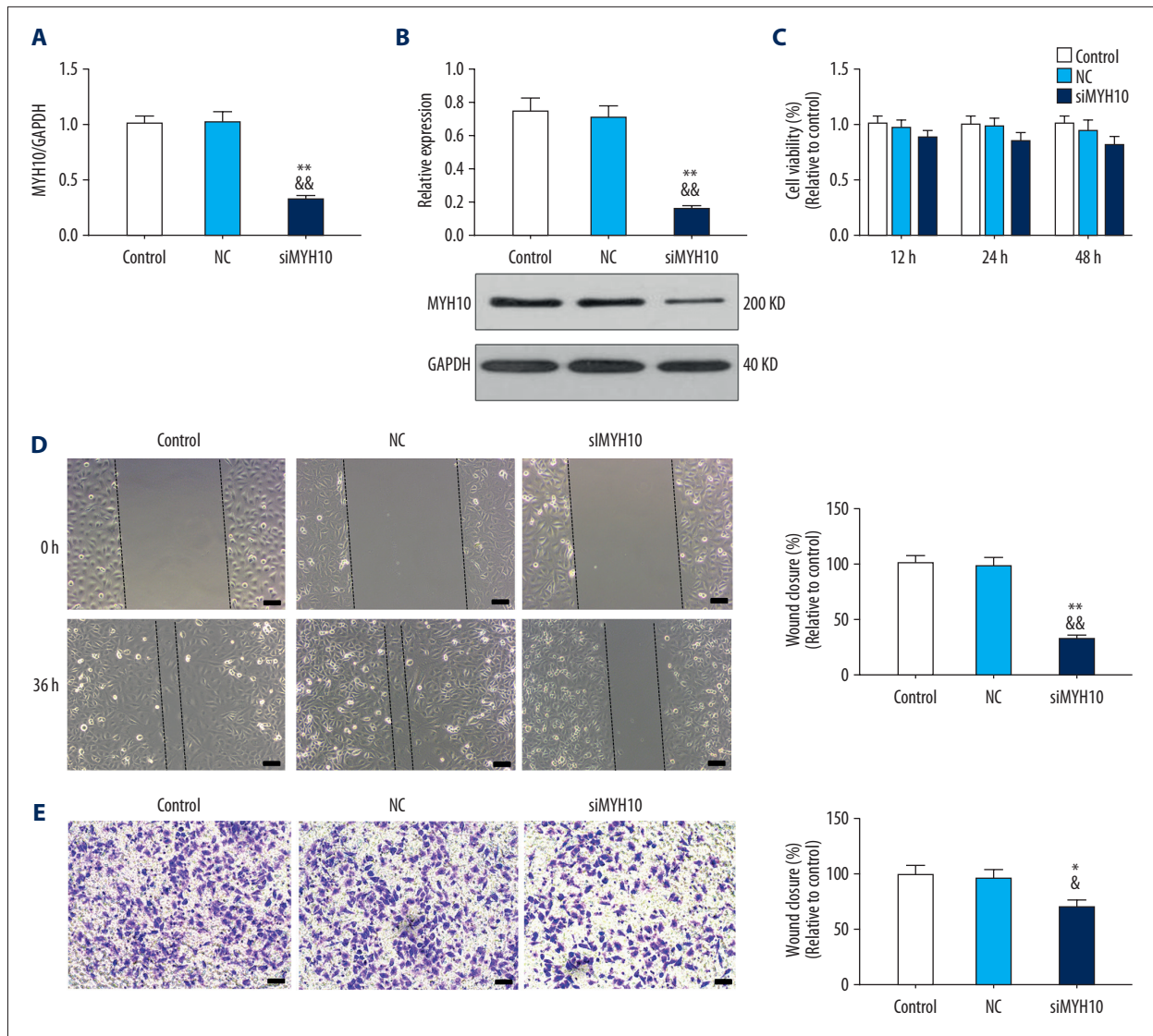
Figure 2. Effects of siMYH10 plasmid interference on the expression levels of MYH10 cell viability, cell motility, and cell invasion of the T98G human glioma cell line. T98G human glioma cells were transfected with phosphate-buffered saline (PBS) (the control group), without the siRNA plasmid (the NC group), and MYH10-siRNA plasmid (the siMYH10 group). (**A**) Quantitative real-time polymerase chain reaction (qRT-PCR) was performed to detect the mRNA level of MYH10 in the different groups. (**B**) Western blot was used to assess the protein level of MYH10 in the different groups. (**C**) Cell viability was analyzed using the cell counting kit-8 (CCK-8) assay. (**D**) The cell scratch test was used to detect cell migration 24 hours after transfection the siMYH10 group). Scale bar, 50 mm. (**E**) The transwell assay was used to detect the rate of cell invasion 24 hours after transfection. Scale bar, 50 mm. * P<0.05, ** P<0.01, compared with the control group; & P<0.05, && P<0.01, compared with the NC group. Data are shown as the mean ±SD (n=4).

MYH10-encoded NM IIB protein is closely related to cell division, cell adhesion, cell migration, and metastasis. The results of the 2006 study by Thiery and Sleeman showed that the MYH10 mutation caused changes in EMT that resulted in decreased cell migration [22]. A previous study has shown that EMT is involved in cell adhesions, contractility, and signaling [23]. The results of this study showed that after the inhibition of MYH10 expression, the migration and invasion of T98G human glioma cells were significantly reduced. Previous studies also

found that NM IIB may play a role in cell adhesion during embryogenesis [24,25]. The presence of NM IIB has been shown to be involved in cell adhesion by maintaining the integrity of the epithelial zonula adherens [26]. In the study by Mai and colleagues, NMIIB was shown to play a role in tumor migration [27]. Therefore, in glioma, the findings that overexpression of the MYH10 gene was associated with invasion and migration of glioma cells, and inhibition of MYH10 gene expression could control the invasion and migration of glioma
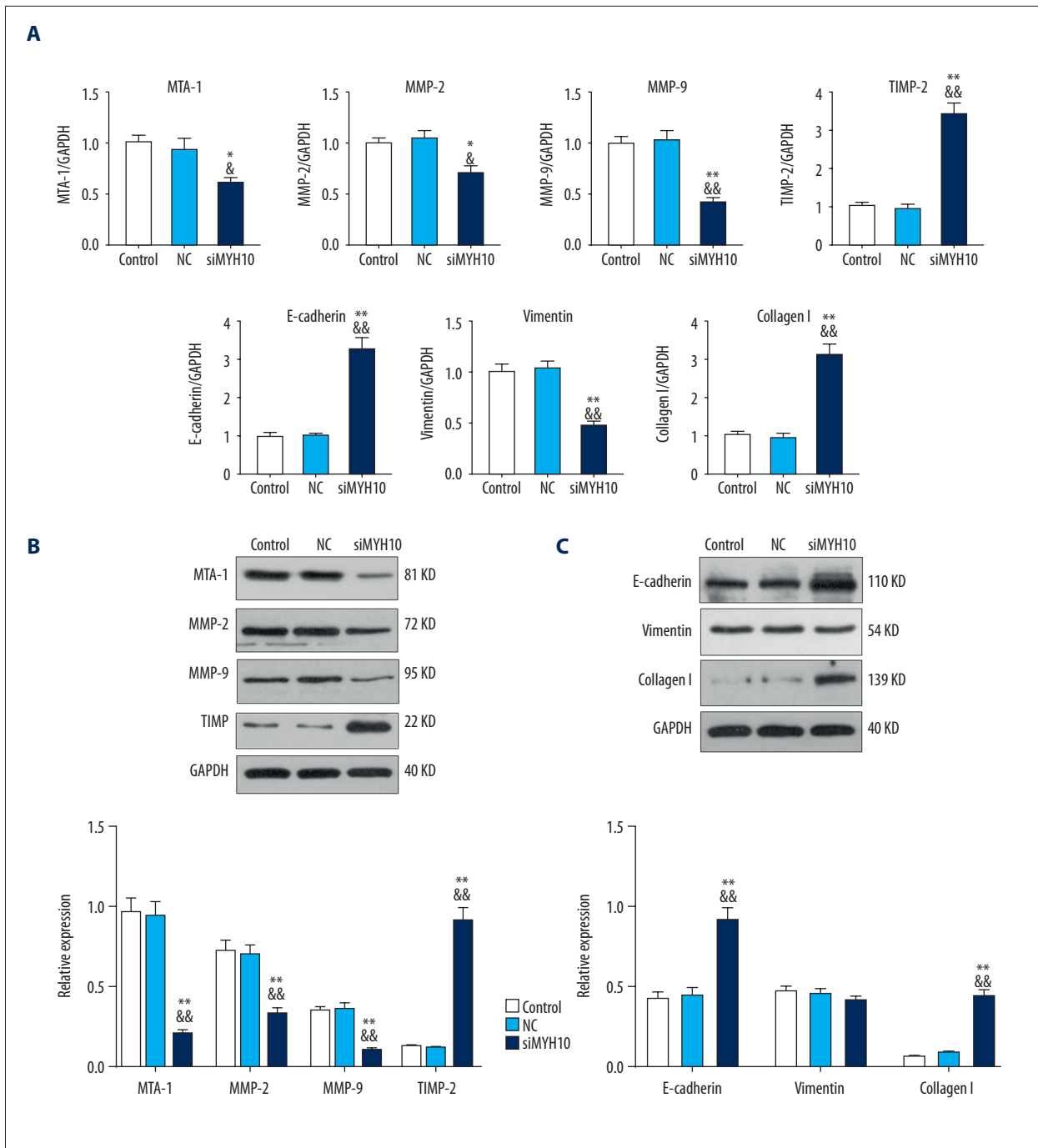
Figure 3. Effects of transfection of siMYH10 plasmid on the expression of epithelial-mesenchymal transition (EMT) and extracellular matrix (ECM)-related genes in the T98G human glioma cell line. (**A**) Quantitative real-time polymerase chain reaction (qRT-PCR) was used to detect mRNA of metastasis-associated protein 1 (MTA-1), matrix metalloproteinase (MMP)-1, MMP-9, tissue inhibitor of metalloproteinases 2 (TIMP2), E-cadherin, vimentin, and collagen I. (**B**) Western blot was used to detect the protein expression levels of MTA-1, MMP-2, MMP-9, and TIMP-2 proteins. (**C**) Western blot was used to detect the expression levels of E-cadherin, vimentin, and collagen I proteins. P<0.05, ** P<0.01, compared with the control group; ^ P<0.05, ^^ P<0.01, compared with the NC group. Data are shown as the mean ±SD (n=4).
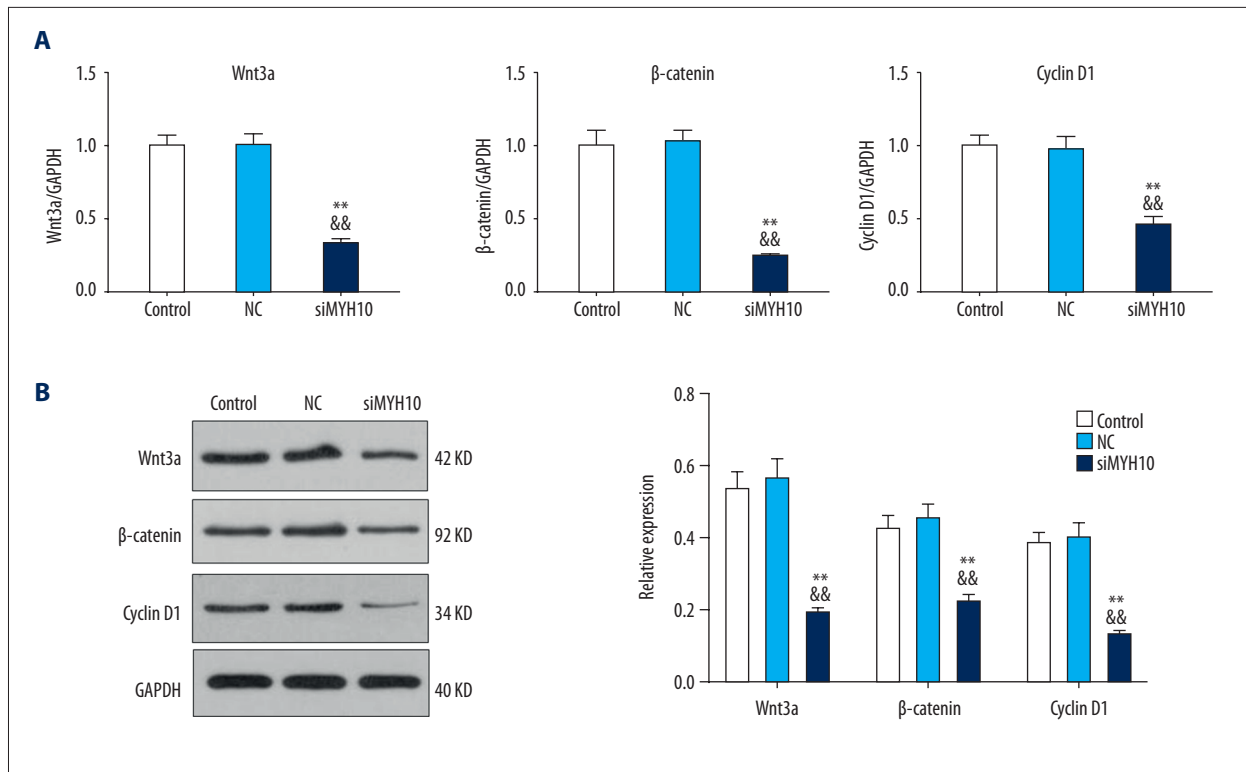
Figure 4. Effect of transfection of siMYH10 plasmid on the Wnt/β-catenin pathway in the T98G human glioma cell line.
(**A**) Quantitative real-time polymerase chain reaction (qRT-PCR) was used to detect mRNA of Wnt3, β-catenin and cyclin D1.
(**B**) Western blot was used to detect the protein expression levels of Wnt3, β-catenin and Cyclin D1. * P<0.05, ** P<0.01,
versus control group; ^ P<0.05, && P<0.01, versus NC group. Data are shown as the mean ± SD (n=4).

cells is supported by findings from previous studies on other tissue and tumor types and requires further study in malignant glioma.

The migration and invasion of malignant cells are related to ECM and EMT processes [28]. E-cadherin, vimentin, and collagen I are common ECM proteins [29,30]. Metastasis-associated protein 1 (MTA-1), matrix metalloproteinase (MMP)2, and MMP9 are important components of the matrix metalloproteinase family, which can hydrolyze intercellular matrix proteins, providing cells with the ability to metastasize [31]. Tissue inhibitor of metalloproteinases 2 (TIMP2) can inhibit MMPs, while increased expression of E-cadherin, vimentin, and collagen I protein stabilize cells [32]. The migration and invasive ability of malignant cells have previously been shown to be associated with overexpression of MTA-1, MMP2, and MMP9 and inhibition of TIMP-2 expression [30–32]. The results of this study showed that after silencing of the MYH10 gene, the expression levels of MTA-1, MMP2, and MMP9 genes and proteins were significantly down-regulated, whereas TIMP-2 was up-regulated. These findings support that in gliomas, silencing the expression of MYH10 has the ability to reduce migration and invasion by increasing the expression of ECM-associated proteins and inhibiting EMT.

Clinical studies have confirmed that Wnt/β-catenin plays an important role in the development, migration, and invasion of cancer cells [33,34]. β-catenin is a key factor in this pathway. The Cyclin D1 gene is a proto-oncogene that maintains cells in the S-phase of cell proliferation resulting in increased cell proliferation [35]. The results of the present study showed that the relative expression levels of Wnt3a, β-catenin, and Cyclin D1 genes in T98G human glioma cells were reduced after MYH10 gene expression was inhibited.

Previous studies have shown that the Wnt pathway regulates the tumor microenvironment and promotes the transformation of epithelial cells and mesenchymal cells into cancer cells, thereby promoting tumor metastasis [36]. The dysregulation of Wnt/β-catenin signaling pathway can increase the migration and invasion of glioma cells [37]. The invasive ability of glioma cells has previously been shown to be reduced by inhibiting Wnt signaling through CBX7 overexpression, and it is possible that dysregulation of Wnt/β-catenin signaling can affect the expression of MMP2, MMP9, E-cadherin, N-cadherin and vimentin, and inhibit EMT and glioma invasion [38]. The Wnt protein includes many subtypes that activate the Wnt/β-catenin pathway, and Wnt3 is just one of these [38]. The Wnt3 protein has the effect of inducing differentiation of mesenchymal

stem cells into neurons, and can also activate proteins in downstream pathways [39, 40]. The extracellular Wnt proteins bind to cell membrane receptors to inhibits the expression of glycogen synthase kinase 3β (GSK-3β), which results in the accumulation of β-catenin in the cell [41]. β-catenin as a critical protein in the Wnt/β-catenin pathway and has a role in tumor migration and invasion, as it can enter the nucleus and promote the expression of Cyclin D1 [42–44]. β-catenin/E-cadherin complexes are formed that promote cell adhesion, and after β-catenin enters the nucleus, it activates the T-cell factor/lymphoid enhancer factor-1 (TCF/LEF-1), which encodes vimentin and MMPs to promote EMT [42–44]. Wnt/β-catenin is also able to promote EMT through the mitogen-activated protein kinase (MAPK) signaling pathway [45]. As a cyclin protein, cyclin D1 overexpression increases cell proliferation, but few studies have been conducted on the role of cyclin D1 expression and cancer metastasis [35,46,47]. Although this was a preliminary *in vitro* study in human glioma cell lines, the findings showed that silencing the MYH10 gene reduced cell migration and invasion, by inhibiting the Wnt/β-catenin pathway, which may regulate the ECM and inhibit EMT in human glioma.

Conclusions

This study has shown that the MYH10 gene is overexpressed in human glioma cells *in vitro*, and that silencing the MYH10 gene reduced cell migration and invasion. These findings might be due to the reduction of extracellular matrix (ECM)-related protein levels and inhibition of epithelial-mesenchymal transition (EMT) by suppressing the Wnt/β-catenin pathway. Further *in vivo* studies should be undertaken to determine whether MYH10 may become a new target for the treatment of malignant glioma.

Conflict of interest

None.

References:

1. Thakkar JP, Dolecek TA, Horbinski C et al: Epidemiologic and molecular prognostic review of glioblastoma. Cancer Epidemiol Biomarkers Prev, 2014; 23: 1985–96

2. Chung DS, Shin HJ, Hong YK: A new hope in immunotherapy for malignant gliomas: Adoptive T cell transfer therapy. J Immunol Res, 2014; 2014: 326545

3. Waghmare I, Roebke A, Minata M et al: Intercellular cooperation and competition in brain cancers: Lessons from Drosophila and human studies. Stem Cells Transl Med, 2014; 3(11): 1262–68

4. Lima FR, Kahn SA, Soletti RC et al: Glioblastoma: Therapeutic challenges, what lies ahead. Biochim Biophys Acta, 2012; 1826(2): 338–49

5. Lim YC, Roberts TL, Day BW et al: Increased sensitivity to ionizing radiation by targeting the homologous recombination pathway in glioma initiating cells. Mol Oncol, 2014; 8(8): 1603–15

6. Conti MA, Adelstein RS: Nonmuscle myosin II moves in new directions. J Cell Sci, 2008; 121(Pt 1): 11–18

7. Wang F, Kovacs M, Hu A et al: Kinetic mechanism of non-muscle myosin IIB: Functional adaptations for tension generation and maintenance. J Biol Chem, 2003; 278(30): 27439–48

8. Sandquist JC, Swenson KI, Demali KA et al: Rho kinase differentially regulates phosphorylation of nonmuscle myosin II isoforms A and B during cell rounding and migration. J Biol Chem, 2006; 281(47): 35873–83

9. Betapudi V, Licate LS, Egelhoff TT: Distinct roles of nonmuscle myosin II isoforms in the regulation of MDA-MB-231 breast cancer cell spreading and migration. Cancer Res, 2006; 66(9): 4725–33

10. Ma X, Takeda K, Singh A et al: Conditional ablation of nonmuscle myosin II-B delineates heart defects in adult mice. Circ Res, 2009; 105(11): 1102–9

11. Nishikawa R, Goto Y, Sakamoto S et al: Tumor-suppressive microRNA-218 inhibits cancer cell migration and invasion via targeting of LASP1 in prostate cancer. Cancer Sci, 2014; 105(7): 802–11

12. Marlar S, Abdellatef SA, Nakanishi J: Reduced adhesive ligand density in engineered extracellular matrices induces an epithelial-mesenchymal-like transition. Acta Biomater, 2016; 39: 106–13

13. Cai J, Guan H, Fang L et al: MicroRNA-374a activates Wnt/beta-catenin signaling to promote breast cancer metastasis. J Clin Invest, 2013; 123(2): 566–79

14. Arend RC, Londono-Joshi AI, Straughn JM Jr., Buchsbaum DJ: The Wnt/beta-catenin pathway in ovarian cancer: A review. Gynecol Oncol, 2013; 131(3): 772–79

15. Huang J, Xiao D, Li G et al: EphA2 promotes epithelial-mesenchymal transition through the Wnt/beta-catenin pathway in gastric cancer cells. Oncogene, 2014; 33(21): 2737–47

16. Lemieux E, Cagnol S, Beaudry K et al: Oncogenic KRAS signaling promotes the Wnt/beta-catenin pathway through LRP6 in colorectal cancer. Oncogene, 2015; 34(38): 4914–27

17. Kole R, Krainer AR, Altman S: RNA therapeutics: beyond RNA interference and antisense oligonucleotides. Nat Rev Drug Discov, 2012; 11(2): 125–40

18. Chang S, Chen W, Yang J: Another formula for calculating the gene change rate in real-time RT-PCR. Mol Biol Rep, 2009; 36(8): 2165–68

19. Shutova MS, Asokan SB, Talwar S et al: Self-sorting of nonmuscle myosins IIA and IIB polarizes the cytoskeleton and modulates cell motility. J Cell Biol, 2017; 216(9): 2877–89

20. Jana SS, Kawamoto S, Adelstein RS: A specific isoform of nonmuscle myosin II-C is required for cytokinesis in a tumor cell line. J Biol Chem, 2006; 281(34): 24662–70

21. Xia ZK, Yuan YC, Yin N et al: Nonmuscle myosin IIA is associated with poor prognosis of esophageal squamous cancer. Dis Esophagus, 2012; 25(5): 427–36

22. Thiery JP, Sleeman JP: Complex networks orchestrate epithelial-mesenchymal transitions. Nat Rev Mol Cell Biol, 2006; 7(2): 131–42

23. Burridge K, Chrzanowska-Wodnicka M: Focal adhesions, contractility, and signaling. Annu Rev Cell Dev Biol, 1996; 12: 463–518

24. Huang Y, Wang X, Wang X et al: Nonmuscle myosin II-B (myh10) expression analysis during zebrafish embryonic development. Gene Expr Patterns, 2013; 13(7): 265–70

25. Ma X, Adelstein RS: A point mutation in Myh10 causes major defects in heart development and body wall closure. Circ Cardiovasc Genet, 2014; 7(3): 257–65

26. Smutny M, Cox HL, Leerberg JM et al: Myosin II isoforms identify distinct functional modules that support integrity of the epithelial zonula adherens. Nat Cell Biol, 2010; 12(7): 696–702

27. Mai J, Qiu Q, Lin YQ et al: Angiotensin II-derived reactive oxygen species promote angiogenesis in human late endothelial progenitor cells through heme oxygenase-1 via ERK1/2 and AKT/PI3K pathways. Inflammation, 2014; 37(3): 858–70

28. Wang L, Wu H, Wang L et al: Asporin promotes pancreatic cancer cell invasion and migration by regulating the epithelial-to-mesenchymal transition (EMT) through both autocrine and paracrine mechanisms. Cancer Lett, 2017; 398: 24–36

29. Du HF, Ou LP, Yang X et al: A new PKCalpha/beta/TBX3/E-cadherin pathway is involved in PLC epsilon-regulated invasion and migration in human bladder cancer cells. Cell Signal, 2014; 26(3): 580–93

30. Garcia-Palmero I, Torres S, Bartolome RA et al: Twist1-induced activation of human fibroblasts promotes matrix stiffness by upregulating palladin and collagen alpha1(VI). Oncogene, 2016; 35(40): 5224–36

31. Jiang Q, Pan Y, Cheng Y et al: Lunasin suppresses the migration and invasion of breast cancer cells by inhibiting matrix metalloproteinase-2/-9 via the FAK/Akt/ERK and NF-kappaB signaling pathways. Oncol Rep, 2016; 36(1): 253–62

32. Li X, Zhou Q, Tao L, Yu C: MicroRNA-106a promotes cell migration and invasion by targeting tissue inhibitor of matrix metalloproteinase 2 in cervical cancer. Oncol Rep, 2017; 38(3): 1774–82

33. Nusse R, Clevers H: Wnt/beta-catenin signaling, disease, and emerging therapeutic modalities. Cell, 2017; 169(6): 985–99

34. Rosenbluh J, Wang X, Hahn WC: Genomic insights into WNT/beta-catenin signaling. Trends Pharmacol Sci, 2014; 35(2): 103–9

35. Luo J, Yan R, He X, He J: Constitutive activation of STAT3 and cyclin D1 overexpression contribute to proliferation, migration and invasion in gastric cancer cells. Am J Transl Res, 2017; 9(12): 5671–77

36. Kato S, Hayakawa Y, Sakurai H et al: Mesenchymal-transitioned cancer cells instigate the invasion of epithelial cancer cells through secretion of WNT3 and WNT5B. Cancer Sci, 2014; 105(3): 281–89

37. Hu T, Xie N, Qin C et al: Glucose-regulated protein 94 is a novel glioma biomarker and promotes the aggressiveness of glioma via Wnt/beta-catenin signaling pathway. Tumour Biol, 2015; 36(12): 9357–64

38. Katoh M: WNT3-WNT14B and WNT3A-WNT14 gene clusters (Review). Int J Mol Med, 2002; 9(6): 579–84

39. De Boer J, Wang HJ, Van Blitterswijk C: Effects of Wnt signaling on proliferation and differentiation of human mesenchymal stem cells. Tissue Eng, 2004; 10(3–4): 393–401

40. Oh SH, Kim HN, Park HJ et al: Mesenchymal stem cells increase hippocampal neurogenesis and neuronal differentiation by enhancing the Wnt signaling pathway in an Alzheimer's disease model. Cell Tansplant, 2015; 24(6): 1097–109

41. Ahmad A, Sarkar SH, Bitar B et al: Garcinol regulates EMT and Wnt signaling pathways *in vitro* and *in vivo*, leading to anticancer activity against breast cancer cells. Mol Cancer Ther, 2012; 11(10): 2193–201

42. Shi Q, Song X, Wang J et al: FRK inhibits migration and invasion of human glioma cells by promoting N-cadherin/beta-catenin complex formation. J Mol Neurosci, 2015; 55(1): 32–41

43. Li H, Wang Z, Zhang W et al: VGLL4 inhibits EMT in part through suppressing Wnt/beta-catenin signaling pathway in gastric cancer. Med Oncol, 2015; 32(3): 83

44. Bastos LG, de Marcondes PG, de-Freitas-Junior JC et al: Progeny from irradiated colorectal cancer cells acquire an EMT-like phenotype and activate Wnt/beta-catenin pathway. J Cell Biochem, 2014; 115(12): 2175–87

45. Gu Y, Wang Q, Guo K et al: TUSC3 promotes colorectal cancer progression and epithelial-mesenchymal transition (EMT) through WNT/beta-catenin and MAPK signalling. J Pathol, 2016; 239(1): 60–71

46. Wang LD, Shi ST, Zhou Q et al: Changes in p53 and cyclin D1 protein levels and cell proliferation in different stages of human esophageal and gastric-cardia carcinogenesis. Int J Cancer, 1994; 59(4): 514–19

47. Qie S, Diehl JA: Cyclin D1, cancer progression, and opportunities in cancer treatment. J Mol Med (Berl), 2016; 94(12): 1313–26